Aircraft Should Not Be Fair Weather Friends – Impact of Winds Aloft on Aircraft Operating Economics

Philip R. Thomas[1]
and
Timothy T. Takahashi[2]

Arizona State University, Tempe, AZ

Aircraft operators and aircraft designers make heavy use of the "deviation method" to account for geographical, weather and temperature differences in atmospheric conditions encountered by aircraft. Standard procedures to estimate en-route aircraft performance rely upon the "standard atmosphere" where real-world conditions are expressed as deviations from this standard. Operators often dispatch based on surface wind and temperature devations at origin and destination airfields and then account for an "average" wind aloft through the concept of an equivalent still air distance. This paper addresses these simplifications with a lateral and vertical weather model incorporated into a point-mass mission simulation that uses real-world atmospheric conditions. We can now determine the effect of changing atmospheric conditions on en-route performance and economy. The custom toolset was used in combination with a series of trades over a range of five days and a representation of each season to show the variation that occurs on a single route over the course of daily and seasonal periods.

I. Introduction

MODERN COMMERICAL AIRCRAFT dispatch using what is known as the temperature deviation method. That is, aircraft performance near an airfield is represented by surface wind velocities and temperature differences based upon a "standard atmosphere" model. Under this paradigm, aircraft designers and aircraft operators begin analysis under assumptions that the atmosphere the aircraft flies through can be modelled using a "standard-atmosphere philosophy", where different properties of the atmosphere can be directly calculated based on pressure altitude [1] [2]. This is even codified under federal law, as 14 CFR 1.1 requires FAA certified aircraft to reference performance to the 1962 U.S. standard atmosphere [3]. However, the real atmosphere may markedly differ from the standard atmosphere. Many flight manuals do not explicitly consider winds, instead they use a method of "equivalent still-air distance" to account for the presence of winds. They also use temperature deviations from the standard atmosphere (ISADEV) to account for all other weather-related atmospheric property changes [4]. These methods are very simplistic; they often make the assumption of a constant ISADEV and seasonal wind averages for calculating fuel consumption and flight fuel economy. This vastly simplifies the real-world conditions, where temperature and winds vary in time through geographical space.

In this work, we ask how should an aircraft best fly when accounting for real-world winds and temperature deviations?

Although the experience of many flight manuals [4][5][6] and traditional literature [7][8] may have one think that the current methods are satisfactory, the advancement of the internet and the rising development of big-data analysis leads us to conclude that there is economic potential to revisit this problem.

We believe that there is little open-literature work that utilizes real-world data, and even less that uses atmospheric data that varies spatially and temporally. Thus, this work sets out to document how aircraft

---

[1] M.S. Candidate, Aerospace and Mechanical Engineering, School for Engineering of Matter, Transport & Energy, P.O. Box 876106, Tempe, AZ, 85287. Member AIAA

[2] Professor of Practice, Aerospace and Mechanical Engineering, School for Engineering of Matter, Transport & Energy, P.O. Box 876106, Tempe, AZ, 85287. Associate Fellow AIAA.

are impacted by both geographic and temporal changes in atmospheric properties.

The University of Wyoming has an atmospheric soundings database that updates twice a day [9]. It provides atmospheric properties such as temperature, humidity, wind speeds, and wind directions from a variety of sounding stations across the world. The main page of the website is shown in FIGURE 1. From a brief perusal of the website, it becomes immediately clear that there is definite variation of atmospheric properties at different stations and at different times, which further supports a need to perform aircraft performance analysis using these real-world datasets. An example of this variation is shown in FIGURE 2, which provides January 2018 wind averages for a variety of sounding stations across the east coast of the United States. We see winds in excess of 50 knots beginning around 15,000-ft and extending as high as 55,000-ft.

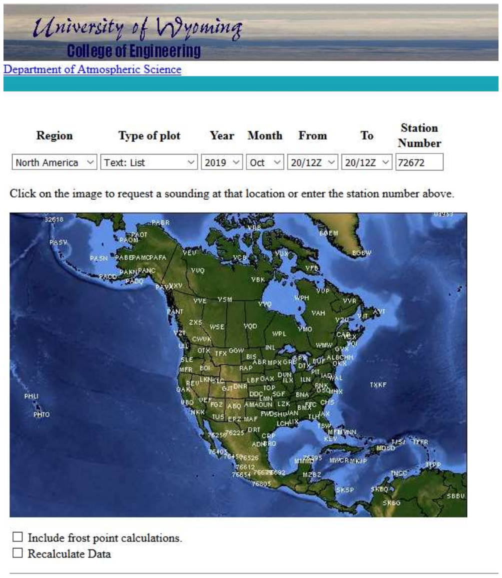

Department of Atmospheric Science

Region	Type of plot	Year	Month	From	To	Station Number
North America	Text: List	2019	Oct	20/12Z	20/12Z	72672

Click on the image to request a sounding at that location or enter the station number above.

☐ Include frost point calculations.
☐ Recalculate Data

Figure 1: University of Wyoming Atmospheric Sounding Database Website [9]

A real-world simulation approach can advise aircraft operators in developing alternative flight plans. Lessons learned from simulating aircraft missions under real-world winds and atmosphere could potentially lead to major changes in recommended cruise altitudes and speeds for aircraft; in future work we will show how attention paid to the jet-stream should influence aircraft conceptual design.

We will see how better understanding winds and temperature deviations aloft can help determine the optimal payload weight. This is because the economy of aircraft is highly impacted by winds; headwinds effectively lengthen a journey while tailwinds artificially shorten it. Understanding how to maximize an aircraft's performance in the presence of changing winds and atmosphere could provide significant improvements to the overall economy of a mission.

Since the maximization of mission economy is a critical goal for all commercial aircraft operators, a large financial incentive exists to develop and perform simulations of aircraft performance with real-world atmosphere models. Even non-commercial operators could benefit significantly from a real-time understanding of aircraft performance, as the winds and atmospheric deviations have a major impact on the true airspeed (TAS), fuel burn and payload capacity, and overall flight dynamics of aircraft.

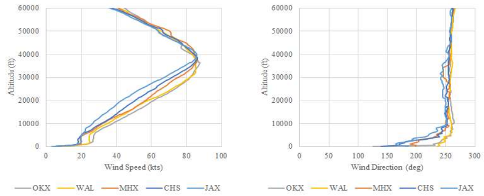

Figure 2: January 2018 Monthly Average Altitude vs Wind Speed and Direction for Sounding Stations along the East Coast

II. Aircraft Performance Model

In this work we will examine the effects of weather upon the mission performance of a notional Airbus *A320* ; see FIGURE 3. This aircraft is a staple in the United States domestic market. It is widely used for narrow-body flights by many major airline operators within the continental United States: JetBlue (130), United (99), Spirit (63), Delta (62) , Allegiant (55), Alaska (53) and American Airlines (48) [11] operate substantial fleets.

Figure 3: Airbus A320 [10]

Different versions of the *A320* feature a wide range of seating options. However, on average the *A320* tends to seat ~150 passengers. This forms the nominal passenger count for the *A320* model used here. A seating chart of a 2019-era Delta Airlines *A320*-200, seating 160 passengers can be seen in FIGURE 4. [12]

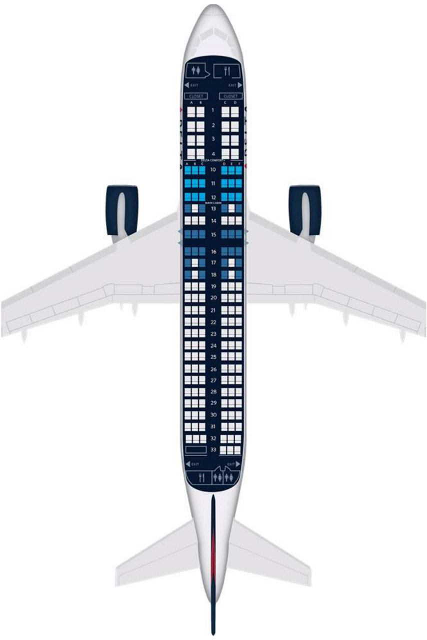

Figure 1: Delta Airlines Airbus A320 Seating Chart [12]

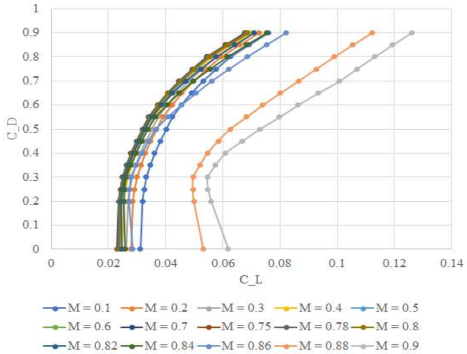

Figure 2: Airbus A320 Drag Polars [14]

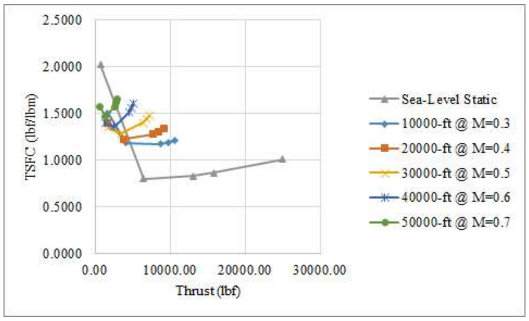

Figure 3: Airbus A320 Power Hook [14]

A well-calibrated aerodynamic and engine model which closely mimics its published performance has been developed in previous research. This provides an accurate basis on which to test the effects of weather on its mission performance [14][15]. The aerodynamics model is based on a nominally-sized *A320* aircraft, with basic wing and fuselage dimensions shown in table 1.

Table 1: Airbus *A320* Dimensions [14]

Item	Value
Wing Reference Area	1319-ft^2
Wing Aspect Ratio	9.17
Wing Quarter-Chord Sweep	25-deg
Wing Taper Ratio	0.24
Fuselage Length	123.25-ft
Fuselage Width	12.95-ft

The physics model of the Airbus *A320* is developed from a combination of its aerodynamics model and engines model. The drag polars of the *A320* form the basis of the aerodynamics data used for modelling the aircraft.

EDET (Empirical Drag Estimation Technique) is a drag estimation code developed by NASA to provide estimations on drag in the conceptual phase of aircraft design [17]. However, prior research has found this method to be suitable to develop aerodynamics databases for real-world aircraft [14][15]. This tool was used to generate the following aerodynamic parameters: lift coefficients (CL) and drag coefficients (CD) at specific angles-of-attack (α) and mach numbers, buffet onset CL at specific mach numbers, and drag corrections at a variety of mach numbers and altitudes.

The drag polars of this model are modelled using an EDET model with excresence drag levels calibrated to match published performance [16], they are shown in FIGURE 5.

NPSS (Numerical Propulsion System Simulation) was also developed by NASA as a programming framework for modelling the mechanical, fluid, and thermodynamic processes within an engine [18]. This tool generates “five-column” thrust data for engines. This dataset includes engine thrust and engine thrust specific fuel consumption (TSFC) at specific altitudes, mach numbers, and power lever (PLA) settings. The engine data and power hooks for each aircraft in chapter 2 were estimated using NPSS.

The engines are modelled as twin 25,000-lbf static reference static thrust, bypass-ratio (BPR) 5 engines [14][15]. Power hooks from this engine data are shown in FIGURE 6.

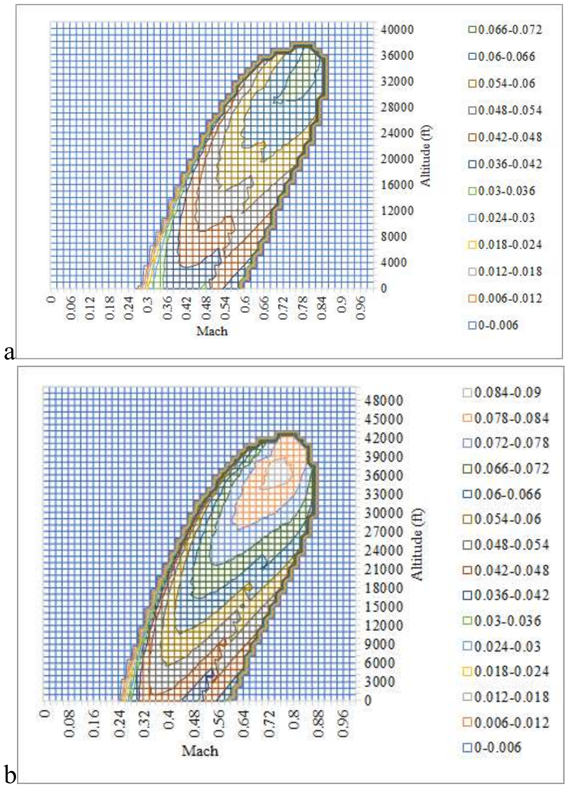

Figure 7 – *A320* Still-Winds Standard-Day Specific Range “SkyMap” nM/lbm-fuel as a function of speed and altitude a) Heavy – W=170,000-lbm; b) Light – W=135,000-lbm

A point-performance “skymap” of specific range as a function of speed and altitude for standard-day conditions in still wind may be found in FIGURE 7 [13]. From the skymaps we can readily see that at light weights (FIGURE 7B), the *A320* is capable of flying at its certified ceiling altitude. However, at heavy weights the *A320* loses much altitude capability to the point that it can barely fly at 38,000-ft (FIGURE 7A). In simper terms, the *A320* cannot fly at its certified flight ceiling when carrying heavy payloads. However, the best specific range can be found at around 36,000-ft for the light weight and around 32,000-ft for the heavy weight, implying that the *A320* flies comfortably below the jet-stream for all configurations.

III. Enroute Aircraft Performance

We used a trade-study approach to investigate the effects of real-world winds and temperature deviations on en-route performance.

For each study, we vary the cruise altitude and takeoff weight of a chosen aircraft to explore change in overall mission fuel and payload economies. Due to the massive variability involved with this field of study, this particular paper focuses on the qualitative and quantitative effects of weather for a single route in still winds, with nominal (seasonal winds) and with actual daily wind patterns.

From an analysis of single route, it is possible to glean how weather impacts domestic flights. This can be used to extrapolate to cover many other routes within reason. Considering that the jet-stream is of primary concern when dealing with winds and that it runs in an easterly fashion, an east-west route was chosen to maximize our analysis of the importance of the jet-stream.

Our chosen route for this thesis simulates flights from the San Francisco bay area to the mid-west. While most operators would actually fly to the Chicagoland area (KORD or KMDR), due to terminal area routing concerns we simplified our mission model to take-off and landing flying a typical route from Oakland, CA (KOAK) to the Quad Cities Airport (KMLI) near Davenport, IA.

The days investigated include a span of five-days in September 2019, as well as a day chosen in each other season (Winter, Spring, and Fall). The five-day series provides an analysis of the effect of day-to-day winds to determine how much an aircraft’s optimal flight conditions change based on daily winds. The seasons provide a broader sense of how the weather impacts the performance of an aircraft over the entire year, providing a sense for the bounds of wind-aircraft interaction.

Six major tools were used for this investigation into real-world en-route flight:

1. EDET (Empirical Drag Estimation Technique), mentioned above

2. NPSS (Numerical Propulsion System Simulation), also mentioned previously

3. A *Lateral Flightpath Generator* – this is a custom tool developed in *Python* to provide *Lateral Navigation* data with real-world weather conditions. The tool allows a user to input a series of waypoints to generate a lateral flight path. It then parses the waypoints from a navigation-weather SQL database and provides interpolated weather data along the requested flight path in 25-nM intervals. The weather data provides weather information for vertical slices of pressure altitudes

from 10000-ft to 51000-ft at each interval. The data itself includes ISA deviations, corrected density altitudes, and wind speeds/directions at each altitude interval and path interval.

4. *Enhanced Skymaps* is an enhanced aircraft point-performance estimation tool that uses EDET files, NPSS files, and wind files to perform a static prediction of aircraft performance over a range of altitude and mach numbers based on an input weight. With a method developed by prior research on point-performance energy-maneuverability, the enhanced version includes the addition of winds and density altitude corrections [19][20] developed by the *Lateral Flightpath Generator* module. This tool was used to prime the vertical *Mission Simulator* by establishing the cruise conditions for an aircraft based upon a weight and altitude by finding the maximum cruise mach number corresponding to 99% best specific range.

5. A non-standard day point-mass *Mission Simulator* is a tool developed in Microsoft Excel/VBA by Dr. Takahashi [20]. This tool provides a full physics simulation of an aircraft depending on a specified vertical mission profile file, EDET file, and NPSS file. The tool uses a time-step integration method where it solves for the combination of lift/drag/thrust parameters to obtain the requested mission profile over time. It closely follows the vertical flight path of the aircraft and solves for all aircraft performance parameters during flight. For this investigation, the tool was modified to include the lateral flight path parameters generated by the *Lateral Flightpath Generator*. As the aircraft "flies" its mission downrange from departure, the mission code will adjust its atmosphere model to account for local deviations in density altitude (for engine performance) as well as account for the winds found aloft.

6. *ModelCenter* is a trade-study tool that provides an interface to link excel workbooks, VBA scripts, and a handful of other programs together with simple logic statements to provide powerful computational investigation with DOE methods. This tool was used to link the various tools together and perform the overall trade studies this thesis is based on.

The *Lateral Flightpath Generator* can be broken down into a series of individual modules that communicate with each other to generate a lateral weather and navigation profile. The modules are: 1) the *Weather Scraper*, 2) the *AeroWinds Database*, and 3) the *Lateral Navigation Engine*.

Figure 8: University of Wyoming weather sounding stations for the continental United States (as seen on http://weather.uwyo.edu/upperair/sounding.html)

At the heart of the weather parsing is an online data scraper that integrates to the University of Wyoming's (UWYO) atmospheric sounding database. This database provides atmospheric soundings twice a day for sounding stations across the world. A map of the sounding stations for North America can be seen in FIGURE 8.

We developed a *Python* script utilizing the *Requests* library and the *BeautifulSoup* library. The script fetches atmospheric data from the UWYO database over HTTP and then parses and converts the data into a usable format for the *Lateral Navigation Engine*.

The UWYO sounding database uses a standardized url format with a series of tags that indicate which specific data is to be fetched. An example request with the tags in bold is shown below:

http://www.weather.uwyo.edu/cgi-bin/sounding?region=**[region]**f&TYPE=TEXT%3ALIST&YEAR=**[year]**&MONTH=**[month]**&FROM=**[startday][starttime]**&TO=**[endday][endtime]**&STNM=**[station number]**

The region tag specifies which region on the world a station is located in. This paper is limited to North America, however further investigations could be made in other regions. The year, month, startday, starttime, endday, and endtime flags indicate the timeframe of data to be requested. The sounding database allows a user to request all data up to a month for a given station. Finally, the station number flag indicates from which station the sounding data is to be obtained.

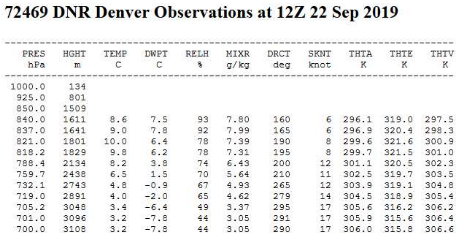

```
72469 DNR Denver Observations at 12Z 22 Sep 2019

-----------------------------------------------------------------------------
   PRES   HGHT   TEMP   DWPT   RELH   MIXR   DRCT   SKNT   THTA   THTE   THTV
    hPa     m      C      C      %    g/kg    deg   knot     K      K      K
-----------------------------------------------------------------------------
 1000.0    134
  925.0    801
  850.0   1509
  840.0   1611    8.6    7.5     93   7.80    160      6  296.1  319.0  297.5
  837.0   1641    9.0    7.8     92   7.99    165      6  296.9  320.4  298.3
  821.0   1801   10.0    6.4     78   7.39    190      8  299.6  321.6  300.9
  818.2   1829    9.8    6.2     78   7.31    195      8  299.7  321.5  301.0
  788.4   2134    8.2    3.8     74   6.43    200     12  301.1  320.5  302.3
  759.7   2438    6.5    1.5     70   5.64    210     11  302.5  319.7  303.5
  732.1   2743    4.8   -0.9     67   4.93    265     12  303.9  319.1  304.8
  719.0   2891    4.0   -2.0     65   4.62    279     14  304.5  318.9  305.4
  705.2   3048    3.4   -6.4     49   3.37    295     17  305.6  316.2  306.2
  701.0   3096    3.2   -7.8     44   3.05    291     17  305.9  315.6  306.4
  700.0   3108    3.2   -7.8     44   3.05    290     17  306.0  315.8  306.6
```

Figure 9 - Sample of the UWYO html sounding file as seen in a web browser

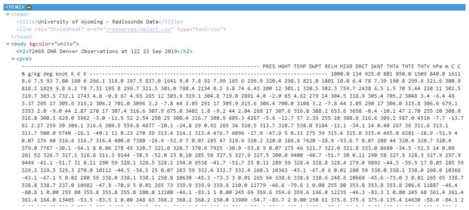

```
<html>
▼<head>
   <title>University of Wyoming - Radiosonde Data</title>
   <link rel="StyleSheet" href="/resources/select.css" type="text/css">
 </head>
▼<body bgcolor="white">
   <h2>72469 DNR Denver Observations at 12Z 22 Sep 2019</h2>
  ▼<pre>
     ----------------------------------------------------------------------------- PRES HGHT TEMP DWPT RELH MIXR DRCT SKNT THTA THTE THTV hPa m C C
     % g/kg deg knot K K K ----------------------------------------------------------------------------- 1000.0 134 925.0 801 850.0 1509 840.0 1611
     8.6 7.5 93 7.80 160 6 296.1 319.0 297.5 837.0 1641 9.0 7.8 92 7.99 165 6 296.9 320.4 298.3 821.0 1801 10.0 6.4 78 7.39 190 8 299.6 321.6 300.9
     818.2 1829 9.8 6.2 78 7.31 195 8 299.7 321.5 301.0 788.4 2134 8.2 3.8 74 6.43 200 12 301.1 320.5 302.3 759.7 2438 6.5 1.5 70 5.64 210 11 302.5
     319.7 303.5 732.1 2743 4.8 -0.9 67 4.93 265 12 303.9 319.1 304.8 719.0 2891 4.0 -2.0 65 4.62 279 14 304.5 318.9 305.4 705.2 3048 3.4 -6.4 49
     3.37 295 17 305.6 316.2 306.2 701.0 3096 3.2 -7.8 44 3.05 291 17 305.9 315.6 306.4 700.0 3108 3.2 -7.8 44 3.05 290 17 306.0 315.8 306.6 679.1
     3353 2.0 -9.0 44 2.87 270 17 307.4 316.6 307.9 675.0 3402 1.8 -9.2 44 2.84 268 17 307.6 316.8 308.2 653.6 3658 -0.4 -10.2 47 2.70 255 20 308.0
     316.8 308.5 629.0 3962 -3.0 -11.5 52 2.54 250 25 308.4 316.7 308.9 605.3 4267 -5.6 -12.7 57 2.39 255 28 308.8 316.6 309.2 587.0 4510 -7.7 -13.7
     62 2.27 259 30 309.1 316.6 309.5 559.8 4877 -10.1 -24.8 29 0.92 265 34 310.5 313.7 310.7 538.0 5184 -12.1 -34.1 14 0.40 267 36 311.6 313.1
     311.7 500.0 5740 -16.1 -40.1 11 0.23 270 39 313.4 314.2 313.4 476.7 6096 -17.9 -47.9 5 0.11 275 39 315.4 315.8 315.4 465.0 6281 -18.9 -51.9 4
     0.07 276 40 316.4 316.7 316.4 400.0 7380 -26.9 -52.9 7 0.07 285 47 319.9 320.2 320.0 386.8 7620 -28.9 -53.6 7 0.07 280 44 320.4 320.7 320.4
     379.0 7767 -30.1 -54.1 8 0.06 278 45 320.7 321.0 320.7 370.6 7925 -30.9 -53.8 9 0.07 275 46 321.7 322.0 321.8 333.0 8680 -34.5 -52.5 14 0.09
     281 52 326.7 327.1 326.8 311.3 9144 -38.5 -52.0 23 0.10 285 56 327.5 327.9 327.5 300.0 9400 -40.7 -51.7 30 0.11 290 58 327.9 328.3 327.9 297.9
     9449 -41.1 -51.7 31 0.11 290 59 328.1 328.5 328.1 294.0 9538 -41.7 -51.7 33 0.11 289 59 328.4 328.8 328.4 279.0 9892 -44.5 -59.5 17 0.05 285 59
     329.3 329.5 329.3 270.0 10112 -44.5 -56.5 25 0.07 283 59 332.4 332.7 332.4 260.1 10363 -43.1 -67.0 6 0.02 280 59 338.0 338.1 338.0 260.0 10366
     -43.1 -67.1 5 0.02 280 59 338.0 338.1 338.1 250.0 10630 -45.3 -73.3 3 0.01 265 64 338.6 338.6 338.6 248.6 10668 -45.6 -73.0 3 0.01 265 65 338.7
     338.8 338.7 237.0 10982 -47.9 -70.9 5 0.01 265 73 339.9 339.9 339.9 210.0 11779 -46.6 -79.6 1 0.00 255 80 353.8 353.8 353.8 206.6 11887 -46.4
     -80.8 1 0.00 255 80 355.8 355.8 355.8 200.0 12100 -46.1 -83.1 1 0.00 245 69 359.6 359.6 359.6 196.0 12235 -46.3 -83.3 1 0.00 245 68 361.4 361.4
     361.4 164.0 13405 -53.5 -83.5 1 0.00 248 63 368.2 368.2 368.2 150.0 13980 -54.7 -83.7 2 0.00 250 61 375.6 375.6 375.6 135.4 14630 -58.0 -84.1 2
```

Figure 10: Sample of the weather html file in raw text as seen from a web browser element inspector

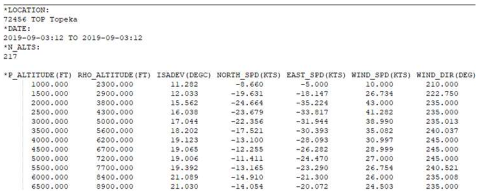

```
*LOCATION:
72456 TOP Topeka
*DATE:
2019-09-03:12 TO 2019-09-03:12
*N_ALTS:
217

*P_ALTITUDE(FT) RHO_ALTITUDE(FT) ISADEV(DEGC) NORTH_SPD(KTS) EAST_SPD(KTS) WIND_SPD(KTS) WIND_DIR(DEG)
     1000.000        2300.000       11.282         -8.660        -5.000        10.000       210.000
     1500.000        2900.000       12.033        -19.631       -18.147        26.734       222.750
     2000.000        3800.000       15.562        -24.664       -35.224        43.000       235.000
     2500.000        4300.000       16.038        -23.679       -33.817        41.282       235.000
     3000.000        5000.000       17.044        -22.356       -31.944        38.990       235.013
     3500.000        5600.000       18.202        -17.521       -30.393        35.082       240.037
     4000.000        6200.000       19.123        -13.100       -28.093        30.997       245.000
     4500.000        6700.000       19.065        -12.255       -26.282        28.999       245.000
     5000.000        7200.000       19.006        -11.411       -24.470        27.000       245.000
     5500.000        7700.000       19.392        -13.165       -23.290        26.754       240.521
     6000.000        8400.000       21.089        -14.910       -21.300        26.000       235.008
     6500.000        8900.000       21.030        -14.054       -20.072        24.503       235.000
```

Figure 11 - Sample weather file generated by the Weather Scraper module

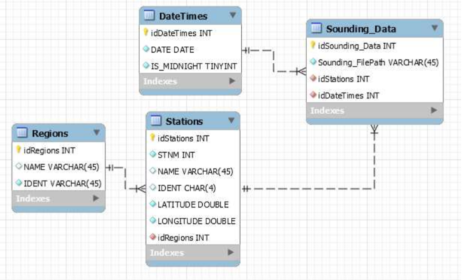

Figure 12 - AeroWinds Database SQL Model

Once this field is provided, the *Weather Scraper* can obtain the webpage html file via the http request. The *BeautifulSoup* module is then used to parse the html file to obtain the weather and station data from the html file. An example of the html file can be seen in FIGURE 9; An example of the html file in raw format can be seen in FIGURE 10.

The file contains tabulated data with eleven columns. However, for our present work we utilized only four columns: these are the HGHT, TEMP, DRCT, and SKNT values which provide information on the geopotential height for a sounding, as well as the atmospheric temperature, wind direction, and wind speed at that height. Absent further information, we conflate geopotential height with the nominal pressure altitude.

Once we obtain the raw data, the *Weather Scraper* standardizes the atmospheric column via linear interpolation along 500-ft intervals, starting with the lowest 500-ft increment up to the highest 500-ft increment all within the scope of the weather data. During this standardization, the *Weather Scraper* converts all units to aviation (i.e. American & British Imperial) units, as this is the customary standard for aircraft performance. The *Weather Scraper* then finally generates a weather file that has all required data. This can be seen in FIGURE 11.

The density altitude conversion is computed from the ISADEV at a corresponding pressure altitude. The particular method used in this thesis is based on an ideal-gas law interpretation of the standard atmosphere, whereby the density of the atmosphere is calculated at a given pressure altitude given a temperature deviation [21]. The temperature deviation is used to identify the pressure altitude corresponding to a matching air density in the standard atmosphere [21]. This results in a density-corrected "equivalent" pressure altitude, hereon stated as the "density altitude" of the atmosphere.

The *AeroWinds Database* module consists of an SQL database of weather files and associated python functions for interacting with the database. The database is designed as a rigid structure to provide access to parsed weather files as requested, allowing a user to quickly obtain weather data based upon a specific station and date/time. A block diagram of this model can be seen in FIGURE 12.

When the user requests data from a station at a certain datetime, the API module first determines whether the data exists in the database. If the weather file is not found, it will fetch the file via the *Weather Scraper* module from the UWYO sounding database. Once the weather file is obtained, the API inserts the file into the database, and provides the user a reference to the file location for further processing.

The *AeroWinds Database* API also includes functions for accessing station latitude and longitude information, which is needed for the *Lateral Navigation* module.

The database prevents identical requests from being sent to the UWYO website and speeds up the overall lateral path generation. By storing parsed data locally, only one request to the UWYO website is needed for each station and day combination. The local files are much quicker to access as the program does not need to wait for the UWYO website before generating the lateral path. This also reduces the network load to the UWYO website, preventing its servers from being overloaded.

The *Lateral Navigation* module generates a lateral path from a series of user-specified waypoints corresponding to the sounding stations in the UWYO sounding database. The module will calculate interpolated weather values along the lateral path legs based on the start and end waypoints for each leg. A sample path with waypoints and legs is shown in FIGURE 13.

Figure 13 - Sample flightpath from OKX to LQC. Waypoints are shown as circles and legs are shown as arrows. Green is the start waypoint and red is the end.

For each leg, the *Lateral Navigation* module splits the distance into 25-nM chunks using a WGS84 ellipsoid model of the earth within the *geographiclib* python library. For each chunk, a vertical profile of winds, temperature deviations, and density altitudes is interpolated from parsed weather data at the start and end waypoints for each leg; see FIGURE 14. The aircraft bearing is also calculated from the latitude & longitude of the start and end waypoints.

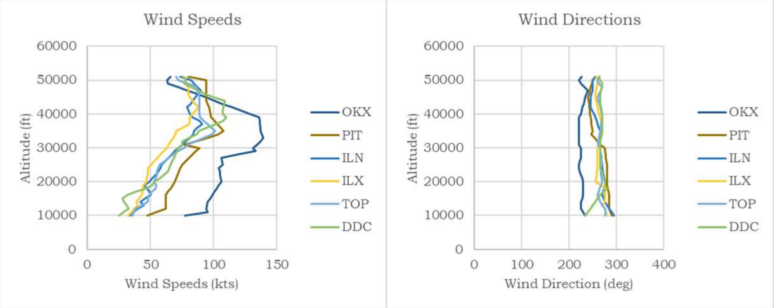

Figure 14 – Headwinds found along a sample flightpath from OKX to LQC.

Once the *Lateral Navigation* module has calculated all intermediary points along the flight path, it compiles the data into a single file for use by the vertical mission simulation tool.

The vertical mission simulation tool calculates the simulation of an aircraft for a specified vertical profile. The profile can be defined by altitude constraints, speed constraints, weight constraints, and more. This is the primary tool used to analyze our aircraft performance with winds aloft. A sample of the main sheet of the tool with a winds-aloft profile can be seen as FIGURE 15.

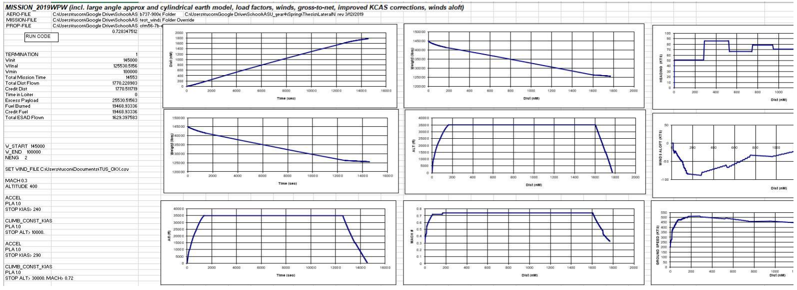
MISSION_2019WPW (incl. large angle approx and cylindrical earth model, load factors, winds, gross-to-net, improved KCAS corrections, winds aloft)

AERO-FILE	C:\Users\tucon\Google Drive\School\AS	b737-900e	Folder	C:\Users\tucon\Google Drive\School\ASU_year4\Spring\Thesis\LateralN	rev 3/12/2019
MISSION-FILE	C:\Users\tucon\Google Drive\School\AS	test_winds	Folder Override		
PROP-FILE	C:\Users\tucon\Google Drive\School\AS	cfm56-7b-e			
	0.728347512				

RUN CODE

TERMINATION	1
Vinit	145000
Vfinal	125530.5156
Vmin	100000
Total Mission Time	14553
Total Dist Flown	1770.228983
Credit Dist	1770.511719
Time in Loiter	0
Excess Payload	25530.51563
Fuel Burned	19468.93336
Credit Fuel	19468.93336
Total ESAD Flown	1629.397583

V_START 145000
V_END 100000
NENG 2

SET WIND_FILE C:\Users\tucon\Documents\TUS_OKX.csv

MACH 0.3
ALTITUDE 400

ACCEL
PLA 1.0
STOP KIAS> 240

CLIMB_CONST_KIAS
PLA 1.0
STOP ALT> 10000.

ACCEL
PLA 1.0
STOP KIAS> 290

CLIMB_CONST_KIAS
PLA 1.0
STOP ALT> 30000. MACH> 0.72

Figure 15 – example of non-standard day mission code output

The simulation tool runs a full physics-based point-mass simulation of an aircraft mission and records the state of the aircraft over time [20]. The tool simulates the vertical mission of the aircraft over time using an Euler-integration method. Each time step, the tool solves all vertical forces and pitching moments acting upon the aircraft. The rates of change for numerous aircraft state variables (fuel burn, weight, etc.) are also calculated during the solution of the forces depending on the requirements (i.e. for cruise thrust must equal drag, and therefore we can determine the fuel flow corresponding to required thrust). Once these are calculated, the aircraft state can then be updated by integrating all relavant forces, velocities, and state rates of change. The vertical mission simulation tool provides the estimated payload, credit distance, total fuel burn, credit fuel burn, total time, and credit time for a given mission. These are used to derive the fuel and payload economies as seen in the Trades Setup section.

IV. Trade Study Setup

We coordinated all mission trade studies using the *ModelCenter* environment [22]; refer to FIGURE 16.

The model begins with the enhanced skymaps excel tool. From the skymaps tool, the target cruise mach number is extracted based upon the input aircraft, weather, and requested cruise altitude [19] [20].

An altitude protection statement in *ModelCenter* prevents the mission simulation from running if the aircraft is incapable of flight at the target altitude and TOW. If this occurs, the run is flagged as invalid in the overall trade study.

Once a run passes the altitude protection statement, it is then passed to a mission distance convergence loop. The vertical mission simulator runs missions where the credit distance is implicitly calculated from an explicit cruise distance.

Thus, we implement a looping structure to alter the cruise distance based upon the credit distance error in order to converge the mission to the target credit distance. The convergence is designed to end when the simulated credit distance is within 10-nM of the target credit distance.

Within the convergence loop, a mission writer script generates the mission file based on the parameters given in the run and those calculated from the skymaps tool. A sample mission file is shown in FIGURE 17. For the purposes of this thesis, we implemented flights with a single cruise altitude (i.e. no step climbs). I n order to ensure that each mission is a legal and proper mission, an additional 100nM divert portion and 45-min hold was added to simulate the extra fuel needed for bad weather as required by 14 CFR 91.167 and 14 CFR 121.639 [3]. This prevents “illegal flights” from being included in the mission and prevents an overestimation of payload capacity.

Once the mission file is generated, it is simulated via the vertical mission simulator. The credit distance, credit fuel, total distance, total fuel, excess payload, and mission time are obtained from the simulator.

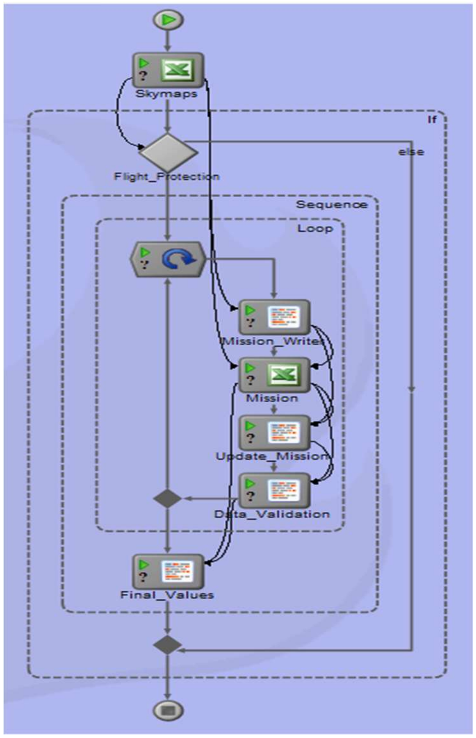

Figure 16: ModelCenter Setup

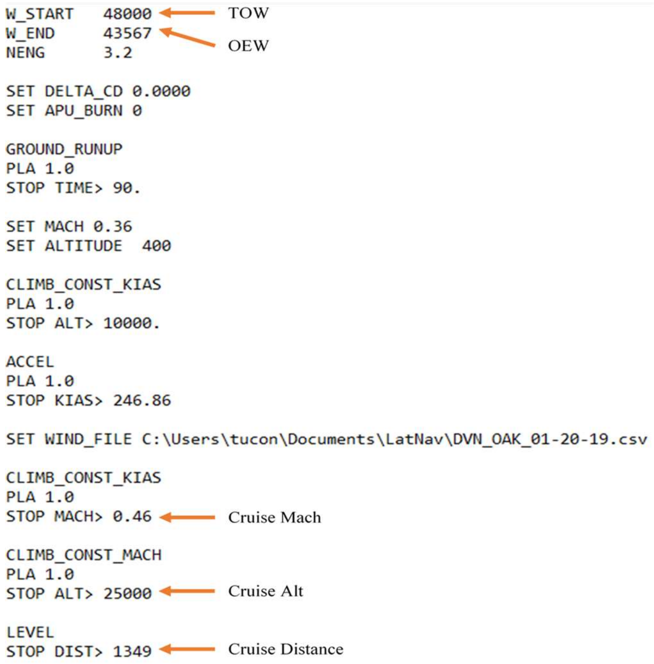

```
W_START    48000
W_END      43567
NENG       3.2

SET DELTA_CD 0.0000
SET APU_BURN 0

GROUND_RUNUP
PLA 1.0
STOP TIME> 90.

SET MACH 0.36
SET ALTITUDE  400

CLIMB_CONST_KIAS
PLA 1.0
STOP ALT> 10000.

ACCEL
PLA 1.0
STOP KIAS> 246.86

SET WIND_FILE C:\Users\tucon\Documents\LatNav\DVN_OAK_01-20-19.csv

CLIMB_CONST_KIAS
PLA 1.0
STOP MACH> 0.46

CLIMB_CONST_MACH
PLA 1.0
STOP ALT> 25000

LEVEL
STOP DIST> 1349
```

Figure 17: Sample Mission file with set winds file

One of the primary metrics used is the average credit specific range, which provides an indication of the fuel efficiency of the target mission. This is calculated by the equation:

$$SR_{Credit} = \frac{CreditDistance}{CreditFuel} \tag{1}$$

A pure payload economy or fuel burn per kilopound-mile (1/1,000-lbm-nM) as:

$$FuelBurnPerKLBMile = \frac{CreditFuel}{CreditDistance \times \frac{ExcessPayload}{1000}} \tag{2}$$

The payload economy determines the cost effectiveness of the mission assuming the total payload can be profit-generating. For the payload perspective, a lower number corresponds to a more “efficient” mission (one that generates the best profit). The specific range is inverted in that a higher number corresponds to a more fuel-efficient mission.

Once *ModelCenter* finishes the vertical mission simulation, the credit distance is compared to the target credit distance in the mission updater script. The mission updater script will update the target cruise distance based on the following formula:

$$NewCruiseDistance = OldCruiseDistance + 0.8 \times DeltaCreditDistance \tag{3}$$

Once the mission has converged, the data validation module will check whether any of the following conditions have occurred:

- Landing Weight > Max Landing Weight (MLW),
- Excess Payload < 0, or
- New Cruise Distance <= 0

If any are true, then the run is flagged as invalid.

After the loop is finished, the final values script performs a final check of all values. If the run is flagged as invalid, then the final values script sets the output values to -1 to prevent contamination of invalid runs.

V. Still Winds performance of a Narrow Body Jet

In order to determine the effect of winds and temperature deviations upon the en-route performance of the *A320* we model baselines uses standard-day en-route performance with still winds.

Here, we vary the take-off weight and the cruise altitude to determine its impact on the fuel economy (*SR*) and payload economy (*FuelBurnPerKlbMile*) of the aircraft. Since there are no winds, there is no difference in the standard condition trades for flying Oakland to or from the Quad Cities.

We show our baseline trade data for the *A320* is shown below in FIGURE 18 to 20. Please note that the *A320* is incapable of flight at weights above a 155,000-lbm takeoff weight at a 40,000-ft initial cruise altitude (FL400), and thus those conditions produce no usable data.

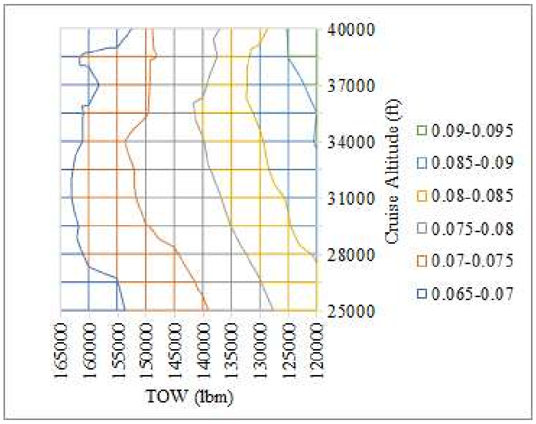

Figure 18: Baseline A320 Credit SR for OAK → MLI

For the *A320*, it appears that the fuel economy of the aircraft is maximized at light TOW and at high altitudes (40,000-ft / FL400). As the TOW increases, the best specific range altitude drops down to ~34000-ft (FL340). This shows an indication that flying above that altitude for heavier weights “overloads” the aircraft too much and brings about an induced drag rise and buffet onset that negates the drag reductions and thrust efficiencies gained from flying at higher altitudes.

From a payload economy perspective as seen in FIGURE 19, it appears that the optimal economy for the *A320* is to seat the maximum number of passengers and take on additional revenue cargo. In this plot, the optimum payload economy is found when flying at the maximum analyzed weight at ~32,000-ft (FL320). This altitude is significantly lower than the 40,000-ft (FL400) flight ceiling of the aircraft, which brings about questions as to the impact of the jet-stream upon the *A320* at its “optimum” payload economy as the jet-stream winds are typically maximized at 40,000-ft (FL400) or higher.

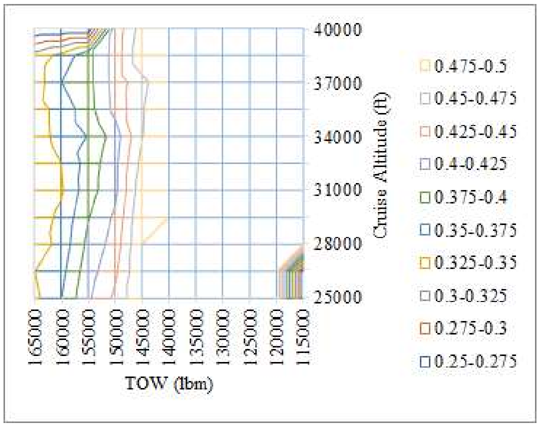

Figure 19: Baseline A320 fuel burn/kilopound-mile for OAK → MLI

The trend of taking more weight as opposed to flying at greater fuel efficiencies is further shown in the overall payload economy of the *A320* in FIGURE 20. In this plot, the optimum payload economy is found when flying at the maximum analyzed weight at ~32,000-ft (FL320).

Looking back at the skymaps for the *A320* (refer top FIGURE 7a and b) in comparison to the baseline economies, we can clearly see the affect of the optimal SR drop as weight increases. At the same low weight (135,000-lbm); the best SR at the heavier weights is also found at ~32,000-ft for both the skymap and overall mission simulation as well. However, the mission simulation provides nuance in the climb, descent, and weight reduction over flight that the skymap does not provide.

IV. Daily Wind Trade Studies

We performed our day-to-day trades using data over a period of 5 days running from September 8, 2019 through September 12, 2019. FIGUREs 20 to 25 show the variation of the weather across each waypoint for each day.

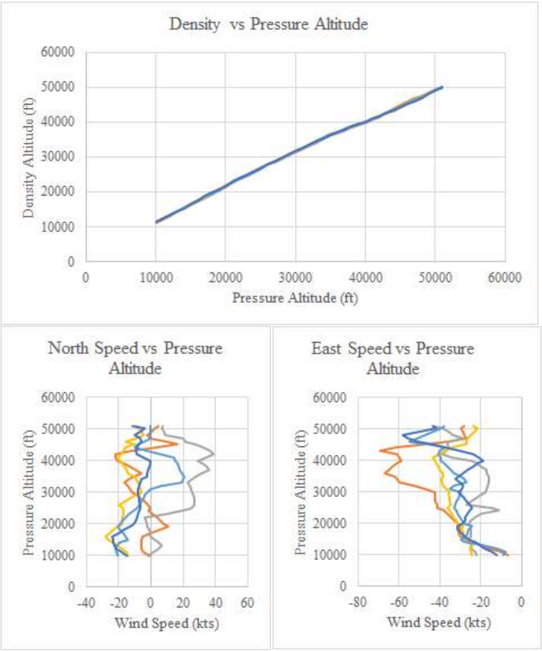

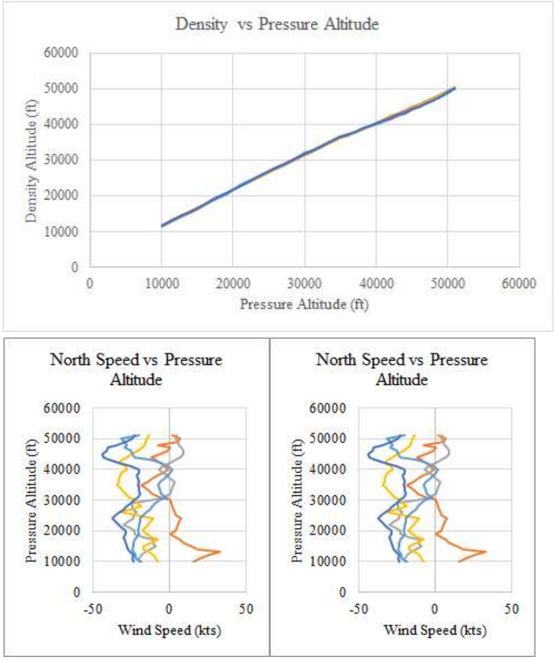

Figure 20: Weather for DVN (Davenport, IA) Station Figure 21: Weather for OAX (Omaha, NE) Station

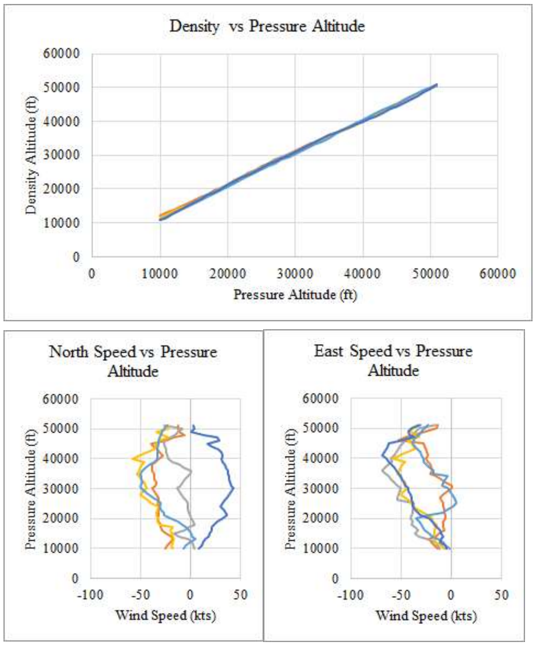

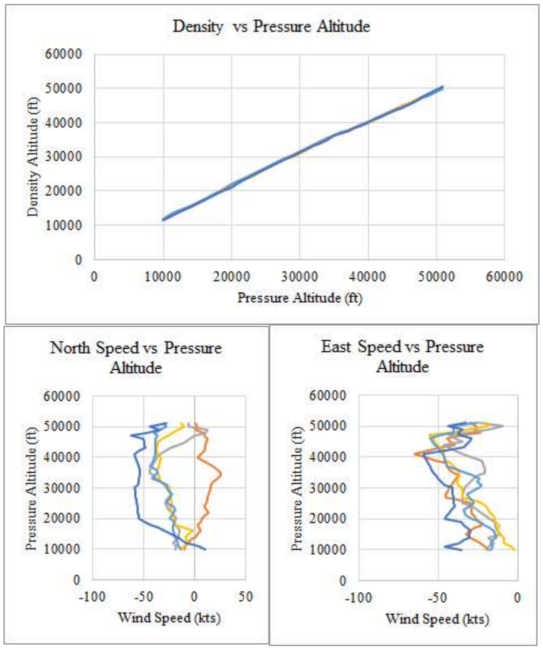

Figure 22: Weather for SLC (Salt Lake City, UT) Station Figure 23: Weather for LBF (North Platte, NE) Station

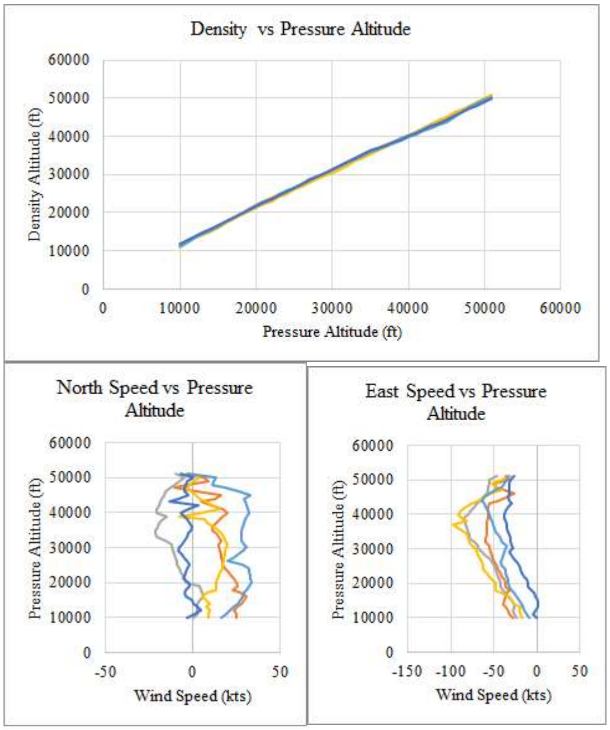

Figure 24: Weather for OAK (Oakland, CA) Station

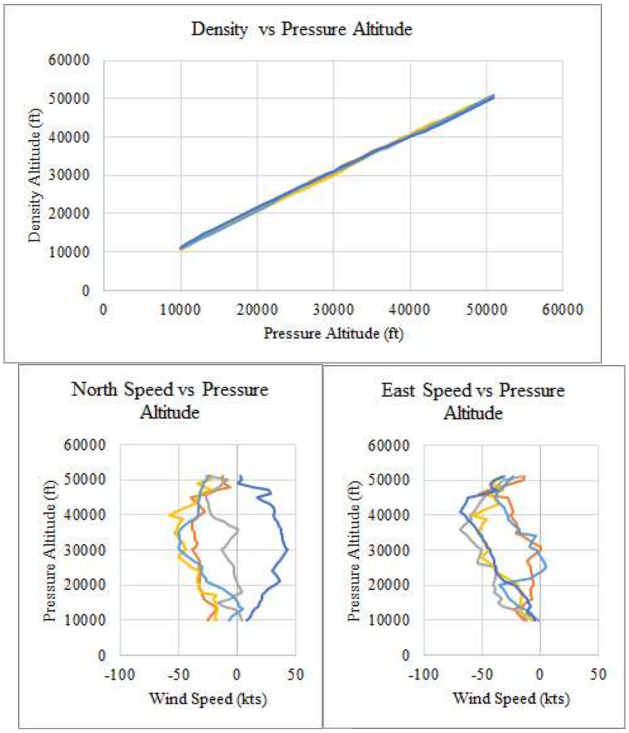

Figure 25: Weather for REV (Reno, NV) Station

From these weather graphs, we can immediately see that the density altitude effects are far less pronounced than the wind effects. Although there is some variation of the density altitudes based on the temperature deviations from ISA over the waypoints, the temperature deviations are small enough in magnitude from each other that the density altitude lines largely line up with each other.

However, winds do have large variation both between each waypoint and from day to day. Although the eastward blowing jet-stream can be seen to peak around 40,000-ft, the precise altitude of maximum winds changes between each station and between each day. This shows that the winds are highly unpredictable between stations and days and provides an initial suggestion that one needs to look at the winds from a daily basis if they are to make the most informed decision about where to fly the aircraft.

A. *A320* Trades: OAK to DVN

The *A320* mission simulations from the above dates for the Eastwards journey have been summarized in the three economies found in the baseline cases. The results for the fuel economy (credit SR) from September 8 to September 12 are shown below in FIGUREs 26 a-e. Note that the aircraft is unable to fly at 40,000-ft (FL400) for TOWs above 155,000-lbm and thus the portion of the SR graphs corresponding to those altitudes and weights are invalid. This applies to all *A320* trades.

We see significant interplay between the winds and the credit specific range. On average, each day the aircraft seems to prefer flying at ~38,000-ft (FL380) to maximize the specific range at lower weights. As the weight increases, the best specific range altitude decreases slowly towards ~33,000-ft (FL330).

So how do the real-world fuel economies compare to the baseline fuel economy? When compared to the baseline fuel economy in FIGURE 18, the fuel economy magnitudes are significantly increased when flying with the winds as compared to the baseline. This is to be expected, as the aircraft gains additional speed from the winds. However, for the most part the altitudes corresponding to the best specific range at each TOW does not change much from the baseline. The largest change can be seen in FIGURE 26a (overleaf) on September 8, 2019, where the best SR at the highest TOW is found at ~35,000-ft (FL350) as compared to the baseline 32,000-ft (FL320). It appears that overloading the aircraft wing by flying at higher altitudes still presents too large an induced drag rise for the *A320* to fly at higher altitudes.

The payload economy (fuel burn/kilopound-mile) of the *A320* can be seen in FIGURE 27a-e.

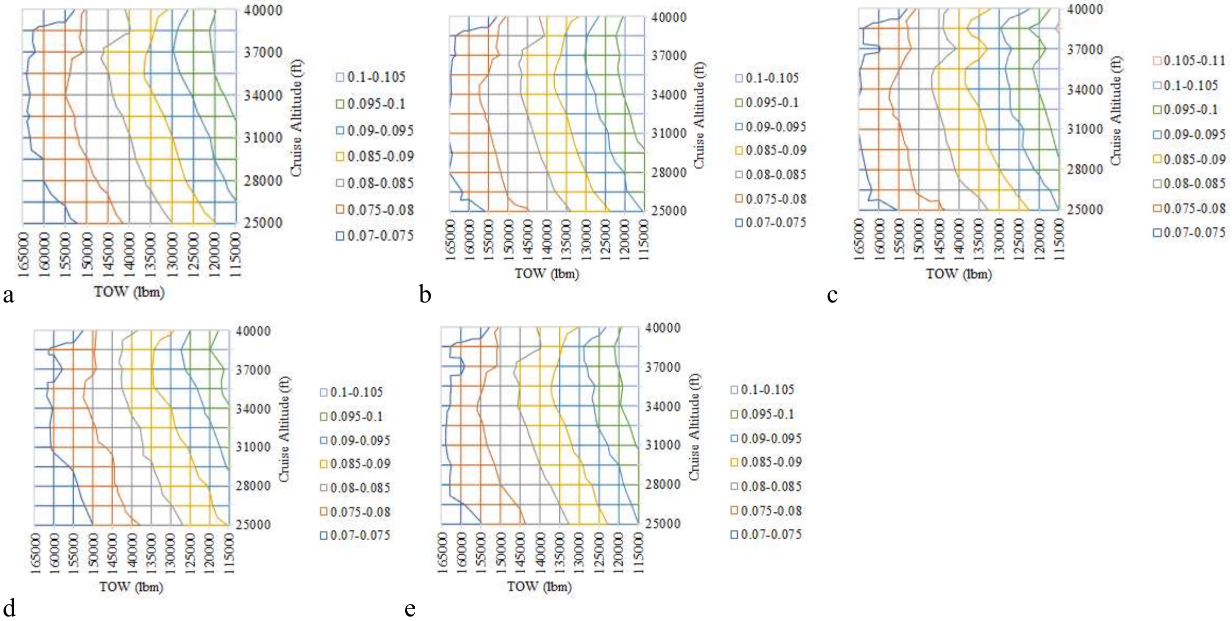

a b c

d e

Figure 26: A320 Credit SR (nM/lbm-fuel) for OAK to DVN on a) 9/8/19, b) 9/9/19, c) 9/10/19, d) 09/11/19, e) 9/12/19

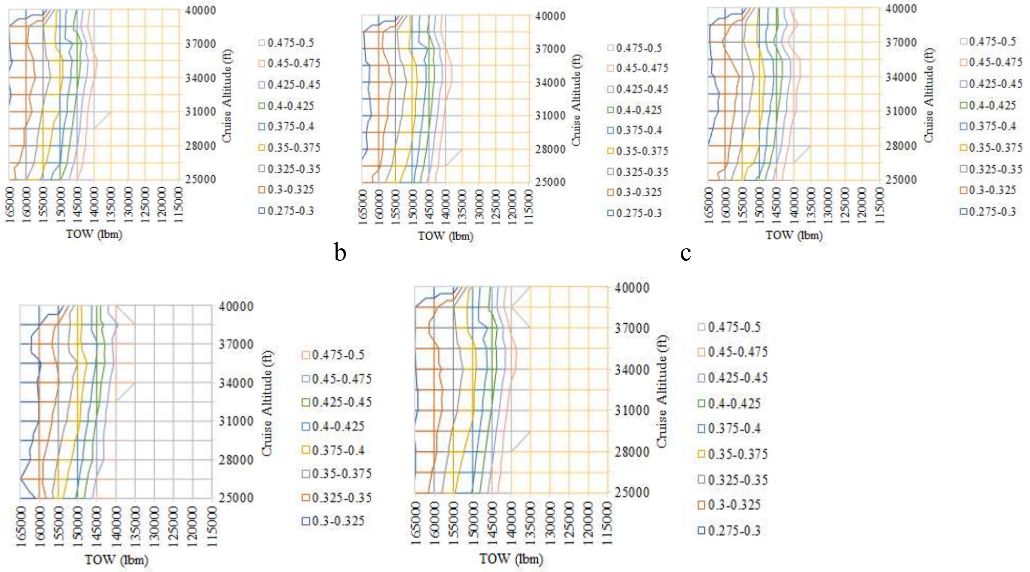

a b c

d e

Figure 27: A320 fuel burn/kilopound-mile for OAK to DVN on 09/10/19

Considering that the maximum wind magnitudes are found at ~40,000-ft (FL400) , it seems that the *A320* is unable to make the most use out of the winds of the jet stream. The induced drag rise and lack of thrust overpowers the benefits of flight at the jet stream. This once again begs the question as to the effectiveness of not only the *A320* but all aircraft that are limited to a 40,000-ft (FL400) ceiling, as it would appear that none of those aircraft would likely be able to fly at altitudes where they can both maximize their passenger load and maximize their use of the jet-stream.

Looking at flight with the jet-stream leads naturally to the corollary of flight against the jet-stream. However, flight against the jet-stream leads to an implicit design philosophy clash: is it better to fly below the jet-stream or above it when flying against the direction of the winds?

B. *A320* Trades: DVN to OAK

When flying against the winds, it can be expected that the *A320* has a net loss in mission economy. When flying with the winds, the aircraft to have the best economies when flying near the jet stream. However, when flying against the jet-stream the aircraft is incentivized to flight away from the jet-stream. This creates two possible options: flight above or flight below the jet-stream.

The *A320* cannot fly above the jet-stream. In theory, this limits its ability to maneuver around the jet-stream winds as it can only get away from the jet-stream by flying below it. However, lower-altitude flight comes with a cost in increasing skin-friction drag. Therefore, the *A320* must balance the impact of the winds against the impact of skin-friction losses.

To get a feel for where the *A320* wants to fly from a day-to-day perspective, we ran the same series of simulations for the *A320* over the week of September 08, 2019 to September 12, 2019 as above. However, this time the flight direction was reversed so that the *A320* flies from Quad Cities to the Bay Area. For these trades, the fuel economy (credit SR) has been plotted in FIGURE 28a-e.

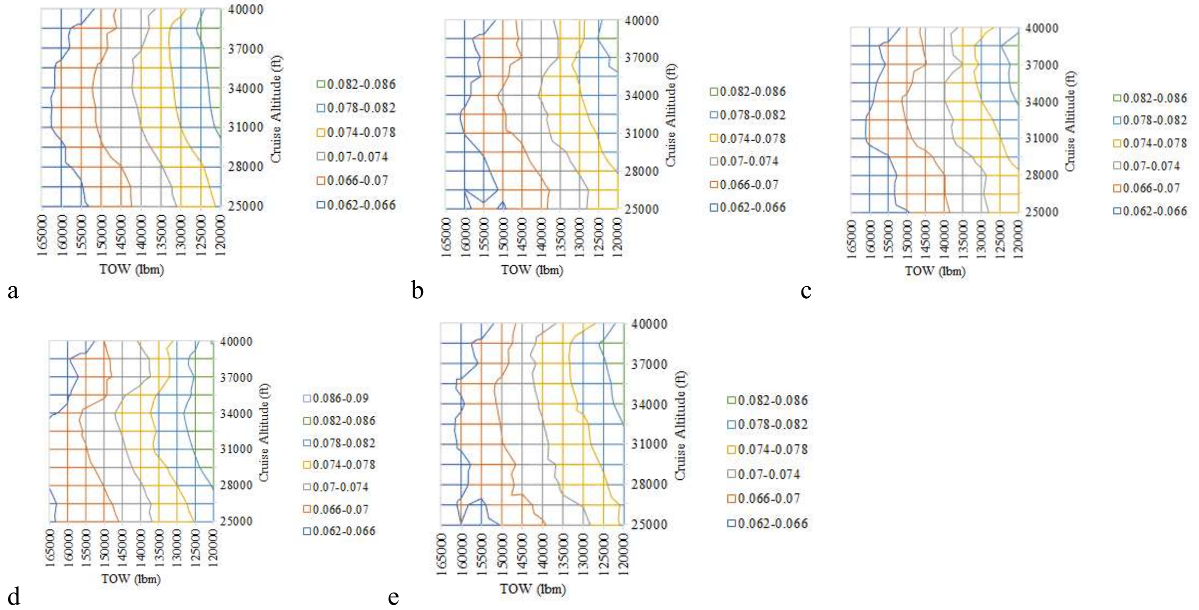

Figure 28: A320 credit SR for DVN to OAK on 09/08/19, 9, 10, 11, 12

From these plots, the impact of the winds is most present at higher altitudes and becomes less impactful at lower altitudes. On the 10th (FIGURE 28c) through the 12th (FIGURE 28e), the fuel economy contours curl back stronger as altitude increases. However, in some cases the contours straighten again at the highest altitude. This curling is likely caused by the interplay between skin-friction drag and winds.

In comparison to flight with the winds in FIGURE 26a-e, the best fuel economy at low weights correspond to lower altitudes when flying against the winds. September 11 (FIGURE 26d) appears to have the most extreme effect where the *A320* has an optimal fuel economy at 34000-ft (FL340) its lowest TOW. This is a 4,000-ft difference from the with-winds flights, where the optimal altitude at low TOWs was found at around 38,000-ft (FL380).

The shapes of the fuel economy curves are also distinctly different as compared to the *A320* baseline fuel economy curve in FIGURE 18. Through flight against the winds, we see a lot of variance both in the shapes of the curves as well as in the gradient of the fuel economy with altitude and TOW. From a qualitative view, it appears that flight against the winds is more variable than flight with the winds.

In order to properly determine the mission economy of the *A320*, the payload economy of the aircraft when flying against the winds must also be determined. Here, we graph the payload economy (fuel burn/kilopound-mile) of the *A320*; refer to FIGURE 29a-e.

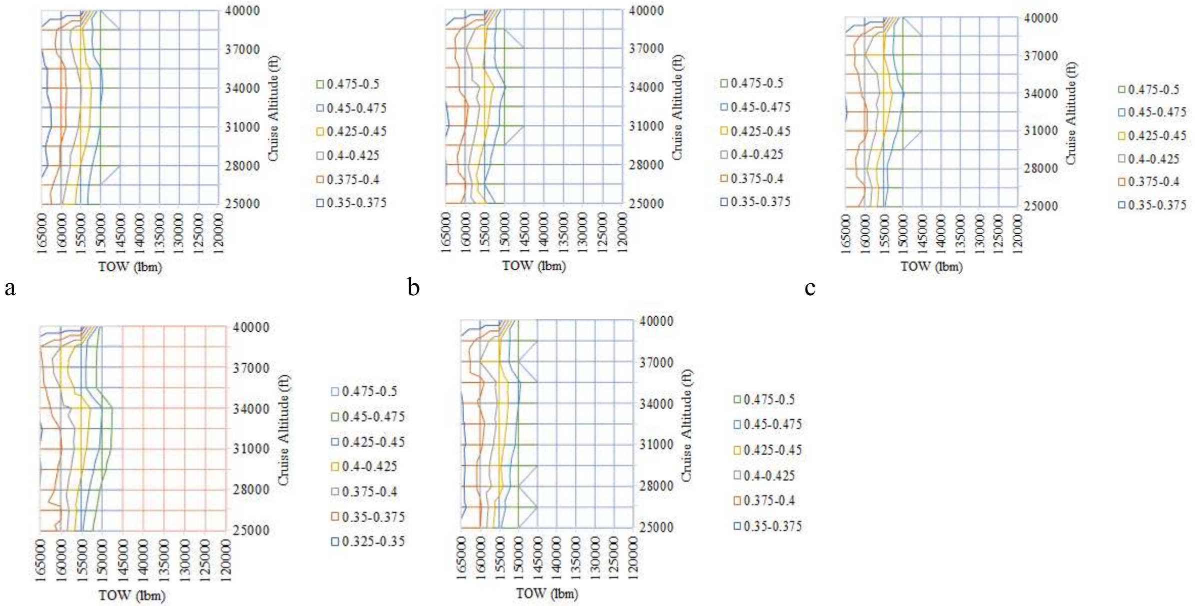

a b c

d e

Figure 29: A320 fuel burn/kilopound-mile for DVN to OAK on a) 09/08/19, b) 9/9/19, c) 9/10/19, d) 9/11/19, e) 9/12/19

Observing the payload economy plots, we see that an optimal payload economy is found at maximum TOW with flight altitudes of ~32,000-ft (FL320). There is some variance between the days, however the impact of the winds seems severely muted (again due to the lower flight altitude of the *A320*). In comparison, flight with the winds has an optimal altitude of ~33,000-ft (FL330). Thus, it appears that the impact of the winds only causes a variation of 1,000-ft on a daily basis for the *A320*. From this initial perspective on winds, it appears that the design of the *A320* has made it inherently resistant to changes in optimal flight conditions based upon winds, because it's drag penalties at flight above and below this altitude both follow rapid expansion that overwhelms the effects of the winds.

The variability of the winds shows up as variance in terms of the shapes of the payload economy contours. From a day-to-day basis, the gradient in terms of altitude and TOW changes quite heavily, where some days the aircraft has a wide range of altitudes corresponding to similar economy, while others it has a narrow region. September 12 (FIGURE 29e) shows a reduction in sensitivity to winds as compared to the 10th and 11th (FIGURE 29c and 29d). On some days, a small switchback also appears at much lower altitudes, and the contours are very rough. For the *A320*, flight against the winds appears to show up as a large amount of "noise" within the graphs that blur our understanding of its performance from its baseline.

C. *A320* Seasonal Trades: OAK – DVN

We have seen that the daily weather variation makes a significant impact upon the operation performance of an aircraft. In this next section we will consider seasonal effects, looking at flights both with and against prevailing winds over a seasonal view. Seasonal atmospheric profiles can be seen for route in FIGUREs 30 to 33, overleaf.

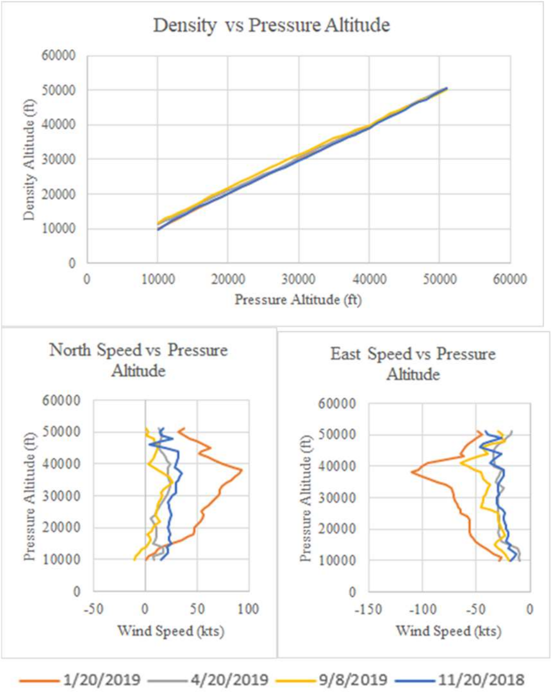

Figure 30: Weather for LBF (North Platte, NE) Station

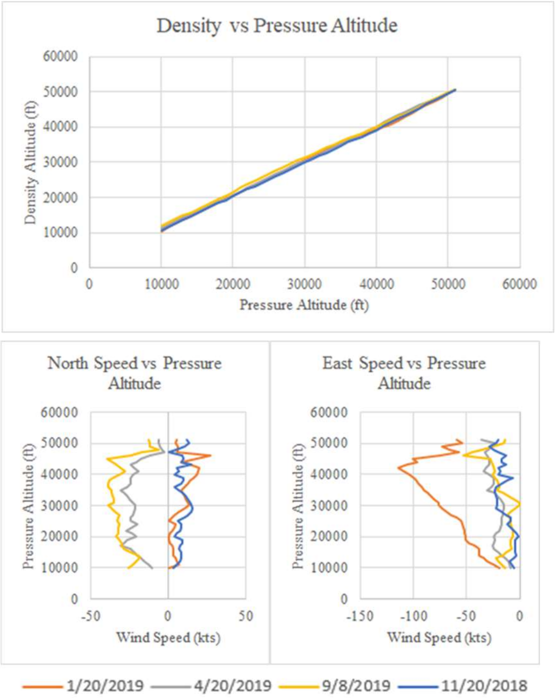

Figure 31: Weather for SLC (Salt Lake City, UT) Station

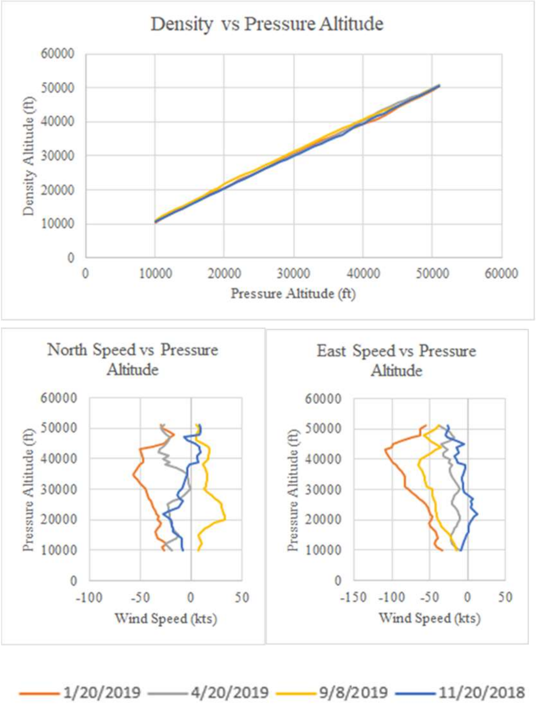

Figure 32: Weather for REV (Reno, NV) Station

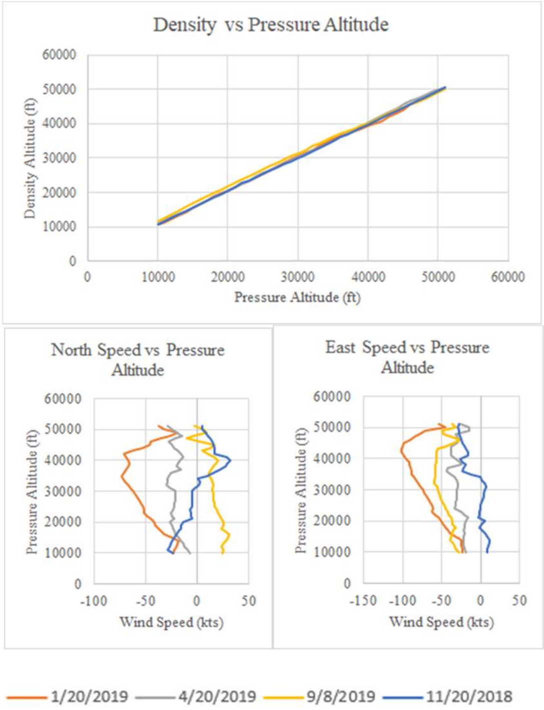

Figure 33: Weather for OAK (Oakland, CA) Station

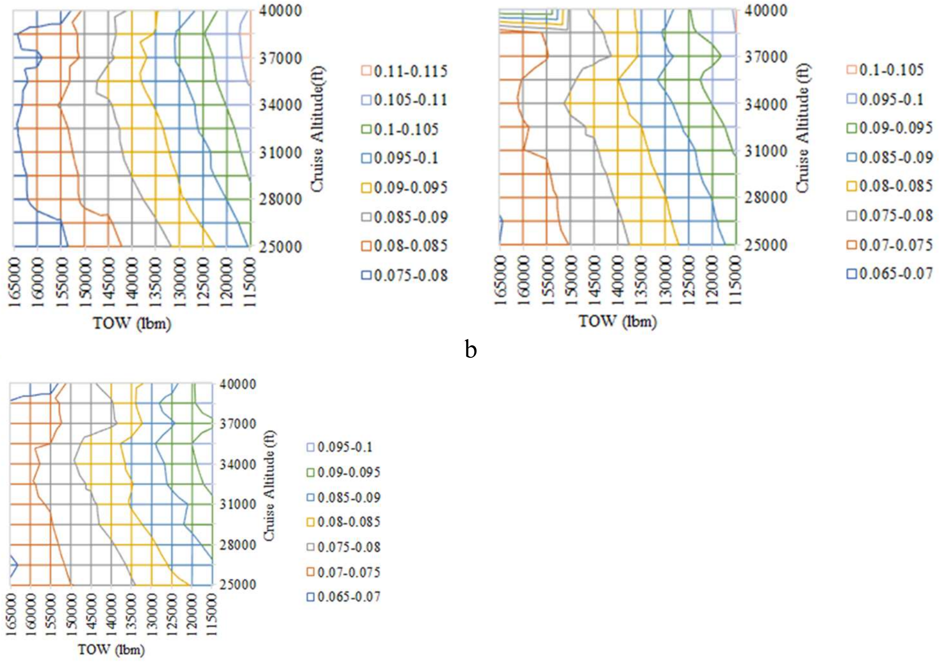

a

b

c

Figure 34: Airbus A320 credit SR for OAK to DVN on a) 01/20/19, b) 4/20/19, c) 11/20/18

For the *A320* in flight with the winds, significant positive impact is seen in January, and less impact in April and November. In the new trades, the impact of the winds is negative rather than positive. In FIGURE 34a to 34c, we plot the fuel economy (credit SR) of the *A320* in flight against the winds on January 20, 2019, April 20, 2019 and November 20, 2018.

From these specific range plots for the *A320*, the trend again appears in that from a fuel economy perspective the aircraft favors the lightest weights and the highest altitude. However, the magnitudes of the specific ranges have ~10% variation between the dates. January shows the best specific ranges reaching between 0.11-0.115 nM/lbm, while November shows the worst specific ranges with a maximum of only 0.9-0.95 nM/lbm. The September plots in FIGUREs 26a to 26e showed an expected maximum specific range of 0.105-0.11 nM/lbm. Considering the wind profiles shown in the seasonal view, it appears that the bi-annual nature shows up in the specific ranges, where the best fuel economy can be expected to occur in the winter and summer months, while the spring and fall months have less fuel economy benefit.

More variation appears in the shapes of the specific range plots as compared to the five-day trade series. The April plot has a small switchback occurring at ~37,000-ft (FL370). Looking at the wind plots, it appears that this may be due to the northerly wind speeds. Since this flight has the *A320* fly in a southwestern direction, northerly winds will have a negative effect on the fuel efficiency of the flight. The northerly winds of the Midwest region have maximum magnitudes around 37,000-ft (FL370), hence the switchback.

There is also a much steeper gradient in terms of the fuel economy in January and September as compared to April and November. Again, this appears to be because of the greater winds in the winter and summer. For the winter and summer months, the winds have a greater magnitude and steeper gradients than in the spring and fall months, hence there is a greater variation of the specific ranges.

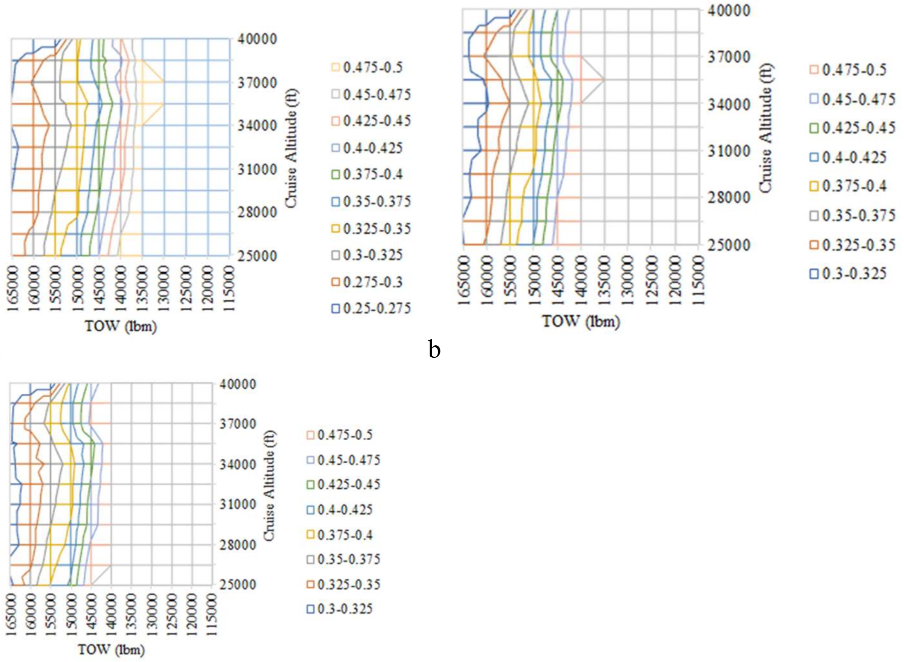

a

b

c

Figure 35: Airbus A320 payload economy for OAK to DVN on a) 01/20/19, b) 4/20/19, c) 11/20/18

The effect of the winds on the payload economy (fuel burn/kilopound-mile) can be seen in FIGURE 35.

Although we already expected that the *A320*'s best payload economy will occur in January (with the strongest winds), there appears to be some significant differences in the cruise altitude upon which the best payload economy can be gained. In January, the *A320* favors 32,000-ft (FL320) or 37,000-ft (FL370) at maximum payload capacity. However, in April the best payload economy can be found at 34000-ft (FL340). In November, the aircraft's best payload economy is found at an altitude of 32,000-ft (FL320). For comparison, the best payload economy for the September 08, 2019 trade can be found at 33,000-ft (FL330).

Considering the maximum and minimum altitudes (37,000-ft / FL370 and 32,000-ft / FL320 respectively), an overall variation of 5000-ft is obtained. This is a significant difference in flight altitudes and suggests that even aircraft such as the *A320* can gain performance and economic benefits from developing flight plans based on the known winds of the route.

D. *A320* Seasonal Trades: DVN – OAK

Here we examine the seasonal trades as with flight with winds, except this time on the return route.

For the *A320* in flight with the winds, significant positive impact is seen in January, and less impact in April and November. In the new trades, the impact of the winds is negative rather than positive. In FIGURE 36a to 36c (overleaf) we plot the fuel economy (credit SR) of the *A320* in flight against the winds on January 20, 2019, April 20, 2019 and November 20, 2018.

The fuel economy plots of the *A320* are far less uniform than in its baseline in FIGURE 18. In January, the overall fuel economy is far worse as compared to its standard day fuel economy. However, the curves are much wider than the standard day and even the other days in this trade. In April and November, the curves are also very jagged in shape. Despite the overall winds being less strong during these months, they appear to add more variability to the economy of the flights, and thus add a lot of noise to the contours of the graphs. In some sense, this means that it may be more important to closely watch the winds in these months as it is more difficult to predict exactly where the optimal altitude might be for fuel economy.

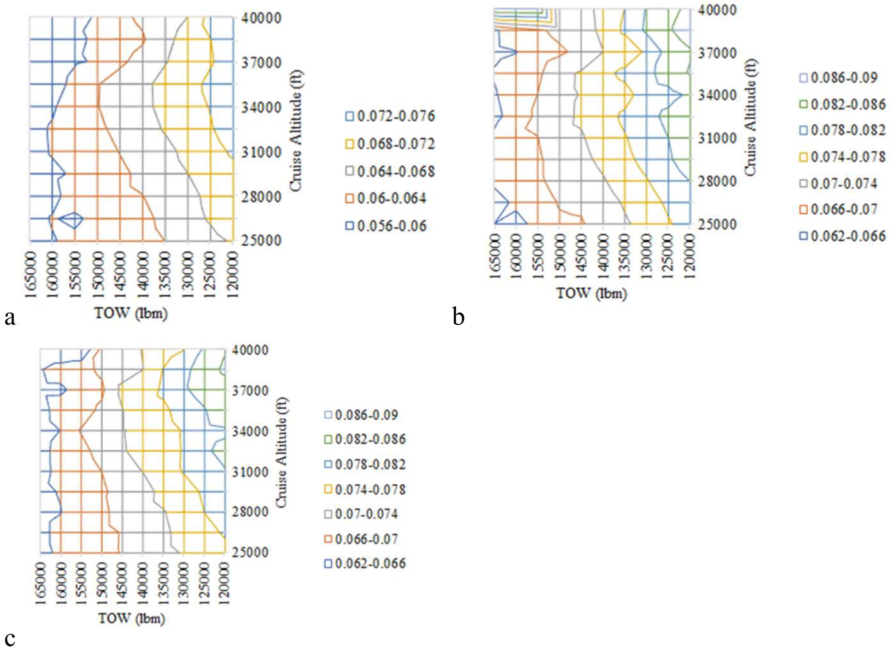

Figure 36: Airbus A320 fuel economy for DVN to OAK on a) 01/20/19, b) 4/20/19, c) 11/20/18

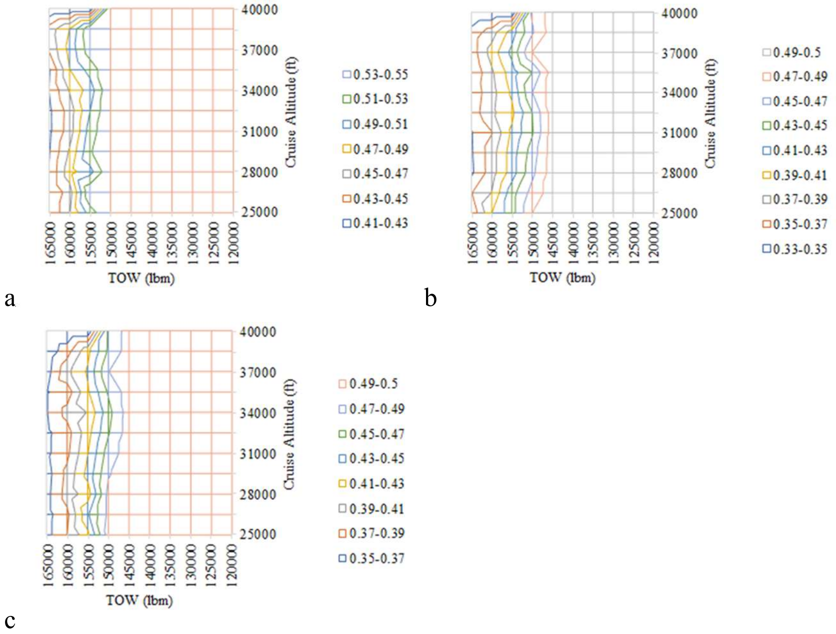

Figure 37: Airbus A320 payload economy for DVN to OAK on a) 01/20/19, b) 4/20/19, c) 11/20/18

In April and November, switchbacks also occur at lighter flight weights at around 34000-ft (FL340). This effect seems to be dampened with increasing TOW, which suggests that the increased induced drag at that altitude begins to dominate the fuel economy decrease over the winds at a TOW of ~140,000-lbm. The best fuel economy altitude also drops heavily as the TOW increases.

The effect of the winds on the payload economy (fuel burn/kilopound-mile) of the *A320* has been plotted in FIGUREs 37a to 37c. Here, we see that the payload economy plots tend to favor flight at lower altitudes. In January, the optimal altitude is found at ~29,000-ft (FL290). In April, the optimal altitude is found around

31,000-ft (FL310), and in November the optimal altitude is at 32,000-ft (FL320). The payload economy plots also seem to be far less sensitive to changes in altitude than to changes in payload, with similar payload economies spanning a wide range of altitudes at high TOWs. As the TOW decreases, more variation in terms of the altitude impact appears, but the direct impact of the winds is still highly muted.

The noise seen in the fuel economy graphs appear to show up again in the payload economy graphs as well in the form of added "jaggedness". Although it is clearer where the optimum flight altitude is located, flight performance on the boundary of these curves becomes hard to predict. Considering the large variability within the tradespace, it presents a strong argument that careful attention to daily winds will allow operators to better predict where they should fly and where they should avoid.

The *A320* appears to have best payload economy when heavily loaded, where the wing appears to be overloaded as compared to its size. This reduces the *A320*'s optimal flight altitude, as any attempt at increasing it would be met with massive increases in induced drag that overshadow the drag benefits from flight in thinner atmosphere.

From the statistical viewpoint, the variability in flight against the winds is much larger than in flight with the winds, especially in the fuel economy and payload economies. The location as to where each data is clustered is also different in each plot based upon the direction of travel. For the fuel economy, the mean is more positive flying against the winds than with the winds. The affect on payload economy is more subtle, but on average it follows the same trend as the fuel economy.

V. Conclusion

From the trades on the Bay Area to Quad Cities region and back, we see how real-world atmospheric conditions add a large amount of variability to the fuel economy and payload economy. This reveals the magnitude of the effect of real-world weather on the performance of aircraft. It also highlights the difficulty in predicting real-world performance from standard day conditions. The effect of winds provides major differences both qualitatively in the shapes of the economy contours, as well as quantitatively with major differences in terms of optimal economy values.

For mission planning, it is clear that flight with the winds provides major benefits as opposed to flight against the winds. However, since the wind speeds, directions, and altitudes will differ from day to day, there is a strong incentive to provide real-time weather updates to predict and optimize the performance of the aircraft. From an operational viewpoint, optimizing flight with the winds has the potential to save up to 20% in terms of the overall payload economy as compared to the flying the design reference mission. In contrast, we see when flying against the winds that there may be as much as a 25% degradation in fuel burn even considering flight at an optimal altitude.

Differences of +/-10% are common depending on flight with or against the winds.

This presents a very strong argument that aircraft operators need to use daily or real-time weather to predict aircraft performance. The variability added by winds and temperature is massive and depends heavily upon the route of travel.

No matter the case, it is deafeningly apparent that winds add a large source of variability to the actual performance of aircraft. Although one may want to think of the winds as either static or static with seasons, it is apparent that the variation on a day-to-day basis develops significant changes in how an aircraft wants to fly. With the rise of interconnected aircraft, increased computation, and an increasing emphasis on big-data approaches to engineering problems, it is clear that the daily analysis of winds should become an industry standard as soon as possible to maximize aircraft performance and mission economy.

Acknowledgements

This manuscript derives from work Mr. Thomas performed in partial fulfillment of the degree requirements for obtaining his M.S. in Aerospace Engineering from Arizona State University. All analysis on this unfunded project was completed at Arizona State University. Professor Takahashi would like the thank Phoenix Integration for their generous academic licensing of *ModelCenter*.

References

1. US Standard Atmosphere, 1962, U.S. Government Printing Office, Washington, D.C., 1962.
2. Sobester, A., Stratospheric Flight, Springer/Praxis Publishing, Chichester, UK, 2011.
3. Code of Federal Regulations, Office of the Federal Register, Washington, D.C., 2019.
4. Anon. *Airbus Industrie A320 Model 320-212 Flight Manual*, Approved by DGAC, Airbus, Blagnac Cedenx, FR, 20 NOV 1990
5. Anon. *737-800 Flight Crew Operations Manual*, Boeing, Seattle, WA, 29 OCT 2008.
6. Anon. *Beechjet (Model 400A) FAA Airplane Flight Manual,* Hawker-Beechcraft Corp., Wichita, KA, 23 OCT 2011.
7. Roskam, J. and Lam, C-T E, *Airplane Aerodynamics and Performance*, Lawrence, KS: DAR Corp., 1980.
8. Anon., *Jet Transport Performance Methods*, Boeing Flight Operations Engineering Training Document D6-1420, Seventh Edition, Boeing, Seattle, WA, 1989.
9. http://weather.uwyo.edu/upperair/sounding.html
10. Linares, A., "Flashback: The Airbus A320 Family", Airways International, 2017.
11. *A320* operator wiki
12. Airbus *A320*-200 Seat Map, Delta Air Lines, Inc., Atlanta, GA., 2019
13. Takahashi, T.T., "Aircraft Concept Design Performance Visualization Using an Energy-Maneuverability Presentation," AIAA 2012-5704, 2012.
14. Beard, J.E. and Takahashi, T.T., "Wind Accountability and Obstacle Clearance Limited Takeoff for Commercial Transport Aircraft," AIAA 2018-3501, 2018.
15. Beard, J.E. "Takeoff Obstacle Clearance Procedures: The Feasibility of Extended Second Segment Climb," Aerospace Engineering M.S. Thesis, Arizona State University, Tempe, AZ, April 2017.
16. WinPEP for A320 (computer software)
17. Feagin, R.C. and Morrison, W.D., "Delta Method, An Empirical Drag Buildup Technique," NASA CR 151971, Lockheed-California Co, Report LR-27975-VOL-1, 1978.
18. NPSS, Numerical Propulsion System Simulation, Software Package, Ver. 2.8, Ohio Aerospace Institute, Cleveland, OH, 2016.
19. Takahashi, T.T., *Aircraft Performance and Sizing, Vol. I: Fundamentals of Aircraft Performance*, Momentum Press, 2016
20. Takahashi, T.T., *Aircraft Performance and Sizing, Vol. II: Applied Aerodynamic Design*, Momentum Press, 2016
21. Takahashi, T.T., Sobester, A., "Climb Performance Anomalies in 'Real' Atmospheric Conditions", AIAA 2019-3271, 2019.
22. ModelCenter, Phoenix Integration, 2019